Indoor Localization Based on Curve Fitting and Location Search Using Received Signal Strength

Bang Wang, *Member, IEEE*, Shengliang Zhou, Wenyu Liu, *Member, IEEE*, and Yijun Mo

***Abstract*—Indoor localization based on received signal strength (RSS) has attracted considerable attention in both academia and industry due to the wide deployment of wireless local area networks. In this paper, we propose a novel indoor localization scheme based on curve fitting (CF) and location search. In the offline phase, we divide the whole environment into some subareas and create a fingerprint for each subarea. We then apply the CF technique to construct a fitted RSS–distance function for each transmitter in each subarea. The online positioning phase consists of two steps. In the first step, we determine a subarea to which a mobile device belongs. In the second step, we propose two location search algorithms, namely exhaustive search and gradient descent search, to find a location within the selected subarea such that the sum of distance errors can be minimized. We conduct field experiments to examine the proposed algorithms. The results show that our algorithms can obtain approximately 20% improvement in localization accuracy compared with the classical fingerprinting-based and lateration-based localization algorithms.**

***Index Terms*—Curve fitting (CF), indoor localization, location search, subarea division.**

I. Introduction

An indoor positioning system helps to obtain the indoor locations of persons, equipment, and materials, which is very useful for various industrial applications, such as construction industry [1], [2], logistics industry [3], and health industry [4], [5]. For example, in [2], indoor localization based on received signal strength (RSS) has been used to provide workers' safety protection in a concrete dam site, In [3], an indoor positioning technique has been applied for multiple asset management in a hospital environment.

Many indoor localization technologies have been developed, which have different hardware requirements and localization performances, such as localization based on Bluetooth [6], [7], ultrasonic [8], [9], radio-frequency ID [10]–[16], ultrawideband [17], [18], and *RSS* [19]–[22]. Among numerous technologies, the one based on the RSS in a *wireless local access network* (WLAN) has become a research focus in recent years. This is because WLANs have been widely used as indoor access systems, and most of mobile devices can easily obtain the RSS information from *access points* (APs) of WLANs.

Lateration and fingerprinting are two main RSS-based indoor localization techniques. The lateration method, however, often suffers from inaccurate distance estimation in indoor environments. For example, it is reported in [23] that the average localization error is about 24.73 ft in a typical office scenario with a width of 80 ft and a length of 200 ft. This is due to two main reasons. One is that the distance estimation based on the log-distance propagation model (PM) is not accurate in complex indoor environments due to the non-line-of-sight (NLOS) problem [24], [25] caused by signal reflection and diffraction. The other is that the lateration-based localization is sensitive to distance estimation error. When one or several distances to APs are not accurately estimated, the localization performance may drop dramatically.

In the recent years, the fingerprinting-based localization has become a hot research topic in indoor localization [26]–[29]. For a given indoor environment, the RSS profiles of some predetermined *reference points* (RPs) with known coordinates are measured, processed, and stored as fingerprints in the offline phase. In the online phase, the RSS profile of a mobile device is compared with those prestored fingerprints to determine its location. The performance of fingerprinting methods is dependent on the number of RP per unit area. It has been reported that increasing the number of RP per unit area helps to improve localization accuracy [26], [30]. However, the RSS measurements are very time-consuming and labor intensive, and using more RPs will much increase the workloads and costs for localization.

In this paper, we propose to apply the *curve fitting* (CF) technique to establish the RSS–distance relation in indoor environments. Instead of using the log-distance PM, we use a series of linearly independent primary functions to construct a general RSS–distance model. The advantage of this method is that it can extract the data change trend from only a few of RSS profiles. Furthermore, we propose to apply the subarea division for CF. In general, the RSS from one AP may be much different in different parts of an indoor environment due to the wall partitions and obstructions, etc. It is not suitable to construct only one fitted curve for the whole area. In this paper, we divide the whole indoor environment into several subareas and construct a fitted RSS–distance curve for each AP and each subarea.

Manuscript received October 12, 2013; revised January 31, 2014, April 3, 2014, and May 4, 2014; accepted May 5, 2014. Date of publication June 2, 2014; date of current version December 19, 2014. This work was supported by the National Natural Science Foundation of China under Grant 61371141.

B. Wang, W. Liu, and Y. Mo are with the Department of Electronics and Information Engineering, Huazhong University of Science and Technology, Wuhan 430074, China (e-mail: wangbang@hust.edu.cn; liuwy@hust.edu.cn; moyj@hust.edu.cn).

S. Zhou was with the Department of Electronics and Information Engineering, Huazhong University of Science and Technology, Wuhan 430074, China. He is now with MEIZU Technology Company, Zhuhai 519000, China (e-mail: zhoushengliang100@126.com).

Color versions of one or more of the figures in this paper are available online at http://ieeexplore.ieee.org.

Digital Object Identifier 10.1109/TIE.2014.2327595

In this paper, we propose a novel two-step localization method. In the first step, we propose subarea fingerprinting to first localize a mobile device to a subarea. In each subarea, we create a subarea fingerprint and construct fitting functions based on the fingerprints of only those RPs within the subarea. In the online positioning phase, we first determine to which subarea a mobile device belongs and then search a space point within the subarea as the mobile device's location. The use of subarea for localization not only helps to reduce the online comparison computations but also to provide a coarse positioning service for those applications with less demanding location requirements.

In the second step, we propose two location search algorithms to find a mobile device's location after the subarea determination, namely exhaustive location search (ELS) and gradient-descent-based location search (GLS). For each subarea, we define an objective function as the sum of distance estimation errors from all available APs. The ELS algorithm is to divide the subarea into many grid points (more than the number of RPs within the subarea) and to search among them a grid point with the least objective value. The GLS algorithm is to iteratively search the global minimizer for the objective function, which utilizes the slope characteristics of the objective function and applies an adjustable step size in the iterative search process.

The proposed scheme improves the RSS-based localization accuracy with reduced workload and can be applied to many industrial applications, such as construction industry, logistics industry, health industry, etc. In short, the contributions of this paper can be summarized as follows.

- We propose a subarea-based CF method for RSS–distance fitting function construction to improve distance estimation accuracy.
- We propose a subarea division and determination strategy to obtain more accurate CF functions and reduce online comparisons.
- We propose a two-step online positioning scheme with subarea fingerprinting and two location search algorithms to satisfy different localization requirements.
- Our field experiments show that, compared with using the traditional PM, the distance estimation accuracy has achieved about 29% improvement by using the subarea-based CF method.
- Our field experiments show that more than 17% and 22% improvements of localization accuracy have been achieved, compared with the traditional fingerprinting method and lateration method, respectively.
- Our field experiments show that the proposed localization scheme has the ability of tolerating environmental changes and device differences. When using one type of device at the offline stage in winter and another type of device at the online stage in summer, our method can also achieve more than 24% improvement of localization accuracy, compared with the traditional fingerprinting method.

The rest of this paper is organized as follows. Section II briefly reviews the related work. Sections IV and V present the offline CF work and online location search work, respectively. In Section VI, we conduct field experiments to verify our algorithm. Finally, we conclude this paper in Section VII.

II. Related Work

Lateration and fingerprinting are two main types of indoor localization methods. The lateration-based localization needs to first obtain estimated distances from a mobile device to multiple APs. The widely adopted radio PM uses a log-distance relation to describe the RSS–distance for distance estimation [23], [31]–[33]. By using some signal samplings obtained at several RPs, the coefficients of the PM can be calibrated. Given an observed RSS, the distance to one AP can be estimated based on the calibrated PM. However, due to the complex indoor propagation environment, the log-distance PM is not accurate, and the distance estimations are often with large errors.

The lateration-based localization is sensitive to the accuracy of estimated distance. When one or several distances are badly estimated, the localization performance drops rapidly. In [25], [34], and [35], the filter techniques, such as the particle filter [25], the Kalman filter [34], and the Bayesian filter [35], have been used to ensure the localization performance, when the distance estimations are with errors. Basically, they apply the previous localization results as guidance information and restrict the possible move traces to limit the localization error. Generally, all these methods need mobile tracking traces.

The fingerprinting-based methods locate a mobile device based on the fingerprint difference between the mobile device's fingerprint and the RPs' fingerprints [26] or the occurrence probability at one location [36]. The performance of these methods are dependent on the number of used RPs per unit area, i.e., the RP density. To relieve the training burden while maintaining the performance, unlabeled data, such as measurements of user casual movement traces, are used to improve the calibration of RSS fingerprints when the training data are insufficient [36]–[38]. Some propose to enrich the RPs by interpolating some virtual points and creating their fingerprints [30], [33], [36]. Generally, these approaches help to reduce the fingerprint calibration efforts, but they are still a discrete scheme with limited fingerprints. In this paper, our proposed GLS algorithm can be conducted in a continuous space, due to the use of fitted RSS–distance functions.

To reduce the online comparison cost, fingerprint clustering methods have been proposed to group RPs into some clusters [39]–[41]. In the online phase, a mobile device is first determined to which cluster it belongs, and then comparisons are only made to those fingerprints within the selected cluster. All these clustering methods are conducted in the signal space, and the RPs in a cluster often form an irregular subarea. Unlike these works, we divide RPs into subareas based on the indoor layout. In this way, a coarse subarea localization result is also useful for applications with fewer demanding location requirements.

III. Preliminaries

Indoor localization can be generally divided into two categories: lateration based and fingerprinting based. In both categories, the localization process consists of two phases: the offline phase and the online phase. In the offline phase, RSSs at

some predefined RPs are first measured, whereas in the online phase, the RSS of a mobile device is collected and used for localization.

Suppose that there are M APs and N evenly distributed RPs in an indoor environment. Let (x_j, y_j) denote the location coordinate of the jth AP, $j = 1, 2, \ldots, M$. For the ith RP, $i = 1, 2, \ldots, N$, let s_{ij} denote its (averaged) RSS from the jth AP, and let d_{ij} denote the Euclidean distance between them. If the jth AP cannot be detected, we simply set a very small value for s_{ij}, e.g., $s_{ij} = -100$ dBm. Furthermore, let $\mathbf{s}_i = (s_{i1}, s_{i2}, \ldots, s_{iM})$ denote the RSS vector at the ith RP in the offline phase. Let $\mathbf{s}^o \doteq (s_1^o, s_2^o, \ldots, s_M^o)$ denote the RSS vector collected by a mobile device in the online phase, and let $\mathbf{s}^o$ be used for the mobile device localization.

For the lateration-based localization, the offline phase is to calibrate some radio PM. The mostly used model is the lognormal shadowing model as follows:

$$\mathrm{PL}(d) = \mathrm{PL}_c + 10\beta \log \frac{d}{d_0} + X(\sigma) \tag{1}$$

where β is the environment attenuation coefficient, d_0 is the reference distance, and $X(\sigma)$ is a zero-mean Gaussian random variable with a standard deviation σ. PL_c is the RSS at the reference distance d_0. The PM is basically an RSS–distance function, mapping from the distance d_{ij} to the received RSS s_{ij}. In practice, only a few of RPs are needed for model calibration. However, since indoor environments are often complex and walls, partitions, and doors greatly affect radio propagation, the calibrated model may not be accurate for distance estimation.

In the online phase, the distances between the mobile device and M APs are first estimated according to the measured RSS vector $\mathbf{s}^o$ and the calibrated PM. The lateration method is then used to determine the mobile device's location based on the least squares principle.

For the fingerprinting-based localization, the offline phase is to collect RSS vectors for all RPs. The RSS vector $\mathbf{s}_i$ is also called the fingerprint of the ith RP, and all the fingerprints are stored in a database. In the online positioning phase, the fingerprint of a mobile device, i.e., $\mathbf{s}^o$, is compared with those prestored in the fingerprint database, and its location is estimated by some localization algorithm. Take the nearest neighbor (NN) in a signal space algorithm as an example. The estimated location $\hat{l}$ is given by

$$\hat{l} = \arg\min_{l_i} \sum_{j=1}^{M} \left(s_{ij} - s_j^o\right)^2, \qquad i = 1, 2, \ldots, N. \tag{2}$$

In general, if more RPs are used, the localization performance can be improved. On the other hand, the workload of offline fingerprint collection and online fingerprint comparison will be much increased, if more RPs are used. Therefore, it is necessary to choose an appropriate set of RPs to balance localization efficiency and performance.

IV. Offline Subarea Fingerprinting and RSS CF

A. Subarea Fingerprinting

In general, the space points that are close in the Euclidean space often experience similar RSSs. This is because the radio propagation environments between these points and the transmitter are similar. Furthermore, in indoor environments, concrete walls have a serious attenuation effect on radio transmission, which often cause several dBm path loss in the RSS. These have been collaborated by our field experiments. Fig. 1 plots the measured RSSs from AP 1 of three selected RPs. The details of our field experiments are introduced in Section VI. In particular, we select RP a and RP b in room 301 and RP c in room 303, as represented by circles in Fig. 2. It is observed that the two RPs in room 301 experience similar RSSs, and the difference of their mean RSSs is about 1 dBm. It is also observed that the mean RSS difference of RPs in different rooms is about 6 dBm, which is mainly caused by concrete wall attenuation. These observations have motivated us to design a subarea-based indoor localization scheme. In this paper, we use some natural building partitions to obtain subareas, such as rooms.

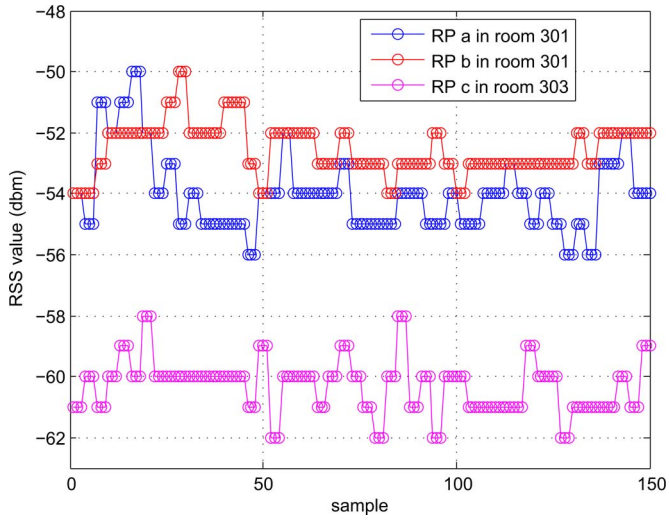

Fig. 1. RSS measurements in our field experiments.

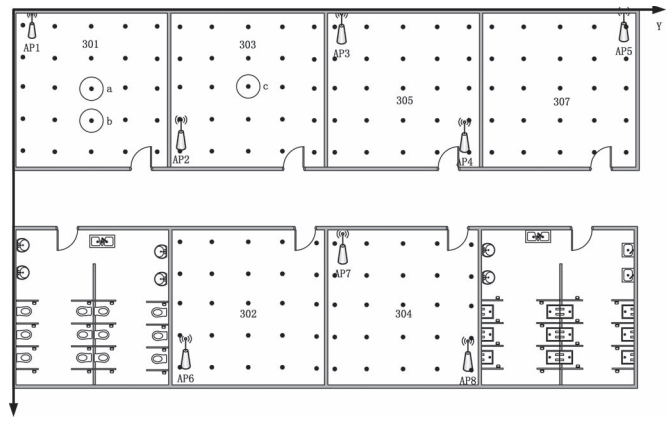

Fig. 2. Third floor of the state engineering laboratory for the next generation of the internet access system. The dots represent the RP locations.

We create a fingerprint for each subarea based on the RSS vectors of RPs within the subarea. Assume that the given indoor environment can be divided into K subareas. All RPs in the kth subarea are grouped into an RP set $\mathcal{R}_k$, $k = 1, 2, \ldots, K$, and we create a subarea fingerprint $F_k = (S_{k1}, S_{k2}, \ldots, S_{kM})$ for each subarea, where S_{kj} denotes the (averaged) RSS from the

jth AP in the kth subarea. The RPs in the same subarea often suffer similar signal propagation; however, their fingerprints differ significantly if they were distributed in different subareas. As such, we simply compute S_{kj} as follows:

$$S_{kj} \doteq \frac{1}{|\mathcal{R}_k|}\sum_{i=1}^{|\mathcal{R}_k|} s_{ij}, \qquad i \in \mathcal{R}_k;\ j = 1, \ldots, M. \tag{3}$$

B. RSS–Distance CF

The objective of CF is to construct a curve (a mathematical function) that has the best fit to a series of data. In this paper, we use CF to build an RSS-distance fitting function to describe the relation between the RSS at some space point and its distance to the transmitter. Compared with the traditional log-distance PM, we do not impose that radio transmission must obey such an exponential path loss and lognormal shadowing. Instead, we propose to build a fitting function by a series of linearly independent primary functions with their coefficients determined by minimizing the fitting error.

We conduct CF in each subarea for each AP. As such, we need to build M RSS–distance fitting functions in one subarea, and $M \times K$ such functions in the whole area. We then introduce how to construct a curve function $\Phi_{kj}(s)$ for the kth subarea and the jth AP, where s is the RSS from the jth AP. For ease of presentation, we drop the subscript, and we let s_i denote the RSS at the ith RP from the jth AP in the kth subarea, and d_i the distance between the RP and the AP. Assume that there are n RPs within the subarea. Note that n may be different in different subareas.

In this paper, we use a group of linearly independent primary functions $(\phi_0, \phi_1, \ldots, \phi_m)$ to build the fitting function

$$d \doteq \Phi(s) = \sum_{h=0}^{m} w_h \phi_h(s), \qquad m < n \tag{4}$$

where m is the fitting degree, and w_h, $h = 0, 1, \ldots, m$, are real-valued coefficients. Note that $\Phi(s)$ is the distance to an AP given the RSS of s. One widely used linearly independent primary functions are $(1, s, s^2, \cdots)$. The sum of squared fitting errors is computed by

$$H = \sum_{i=1}^{n} \left[d_i - \Phi(s_i)\right]^2. \tag{5}$$

Based on the least squares principle, H should be minimized. H is a quadratic function about variable w_h and can be rewritten as

$$H(w_0, w_1, \ldots, w_m) = \sum_{i=1}^{n}\left[d_i - \sum_{h=0}^{m} w_h \phi_h(s_i)\right]^2. \tag{6}$$

To minimize H, we equate its partial derivatives to zero with respect to each coefficient w_h

$$\frac{1}{2}\frac{\partial H}{\partial w_j} = \sum_{i=1}^{n} \phi_j(s_i)\left[d_i - \sum_{h=0}^{m} w_h \phi_h(s_i)\right] = 0. \tag{7}$$

For convenience, we introduce the inner product as follows:

$$(\phi_a, \phi_b) = \sum_{i=1}^{n} \phi_a(s_i)\phi_b(s_i), \qquad a, b = 0, 1, \ldots, m.$$

Then, (7) can be converted into the matrix format as follows:

$$\underbrace{\begin{bmatrix} (\phi_0,\phi_0) & \cdots & (\phi_0,\phi_m) \\ (\phi_1,\phi_0) & \cdots & (\phi_1,\phi_m) \\ \vdots & & \\ (\phi_m,\phi_0) & \cdots & (\phi_m,\phi_m) \end{bmatrix}}_{U} \underbrace{\begin{bmatrix} w_0 \\ w_1 \\ \vdots \\ w_m \end{bmatrix}}_{W} = \underbrace{\begin{bmatrix} (\phi_0, D) \\ (\phi_1, D) \\ \vdots \\ (\phi_m, D) \end{bmatrix}}_{V} \tag{8}$$

where $D = (d_1, d_2, \ldots, d_n)^T$, and $(\phi_h, D) = \sum_{i=1}^{n} \phi_h(s_i) d_i$. The fitting coefficients $W = [w_0, w_1, \ldots, w_m]^{tr}$ can be computed by

$$W = U^{-1}V. \tag{9}$$

V. Online Subarea Determination and Location Search

In this section, we propose a new online positioning method, which consists of two steps: subarea determination and location search.

A. Subarea Determination

The objective is to choose a subarea to which the mobile device belongs, such that the location search is only performed within the chosen subarea. In this paper, we use the nearest neighbor in signal space for subarea determination. The mobile's fingerprint $\mathbf{s}^o \doteq (s_1^o, \ldots, s_M^o)$ is compared with those subarea fingerprints F_k, $k = 1, 2, \ldots, K$, and the subarea with the minimum fingerprint difference is selected. For the kth subarea, the fingerprint difference is computed by

$$D_k \doteq \|F_k - \mathbf{s}^o\| = \sqrt{\sum_{j=1}^{M}\left(S_{kj} - s_j^o\right)^2}. \tag{10}$$

The subarea with the minimum D_k is selected.

B. Location Search

Suppose that the kth subarea is selected in the first step. In the second step, we search a space point $(\hat{x}, \hat{y})$ within the selected subarea, such that the sum of distance estimation error for each AP could be minimized. That is

$$(\hat{x},\hat{y}) = \arg\min_{(x,y)} J \equiv \sum_{j=1}^{M}\left(\Phi_{kj}(s_j^o) - \sqrt{(x_j - x)^2 + (y_j - y)^2}\right)^2 \tag{11}$$

where Φ_{kj} is the RSS–distance fitting function of the jth AP in the kth subarea, and $\Phi_{kj}(s_j^o)$ is the estimated distance between the mobile device and the jth AP. In this paper, we propose two methods to conduct location search: exhaustive search and gradient descent search.

1) Exhaustive Search: In the exhaustive search, we use a grid lattice to represent a subarea. For each grid point, we compute its J value according to (11), and the grid point with the smallest J value is used as the mobile device's location. Obviously, this method is of high computation complexity if the grid step size is small. On the other hand, a smaller step size may help to improve the localization accuracy as the space is described finely. In this paper, we choose a step size of 0.1 m for a typical office scenario.

2) Gradient Descent Search: This method is to iteratively search a location $l \equiv (x, y)$ to reduce $J(l)$ in each iteration. Let $l^{(t)}$ denote the location in the tth iteration, $t = 0, 1, 2, \ldots$. The search iteration is defined by

$$l^{(t+1)} = l^{(t)} + \alpha^{(t)} \times d^{(t)} \tag{12}$$

where $\alpha^{(t)}$ is the search step size and $d^{(t)}$ is the search direction, respectively. Generally, the search step size can be a constant or an adjustable value. To achieve a better performance, in this paper, we allow an adjustable search step size.

Determine $l^{(0)}$: $l^{(0)}$ is the initial location of the iterative search process. Generally, it can be randomly selected. However, a random one may require numerous iterations and even falls into local minima in some cases. To improve the search efficiency, in this paper, we set the initial point as the NN localization result in the target subarea (this localization scheme is also called SD-NN method which will be introduced in Section VI).

Determine $d^{(t)}$: For the function $J(l^t)$, the gradient at the location $l^{(t)}$ is computed by

$$\nabla J\left(l^{(t)}\right) = \left[\frac{\partial J\left(l^{(t)}\right)}{\partial x}, \frac{\partial J\left(l^{(t)}\right)}{\partial y}\right]^{\mathrm{tr}}$$

and its direction is the fastest growth direction of $J(l^{(t)})$. Therefore, to reach the minimum point of $J(l)$ quickly, the negative gradient direction is used as the search direction. That is, $d^{(t)} = -\nabla J(l^{(t)})$.

Determine $\alpha^{(t)}$: Given the search direction $d^{(t)}$ in the tth iteration, then in the $(t+1)$th iteration, $J(l^{(t+1)})$ becomes a function of $\alpha^{(t)}$. We adopt the Golden Section method [42] to obtain $\alpha^{(t)}$, which satisfies

$$\alpha^{(t)} = \arg\min_{\alpha} J\left(l^{(t)} - \alpha \nabla J\left(l^{(t)}\right)\right). \tag{13}$$

The Golden Section method is a 1-D optimization method. It works as follows: Insert two points a_1 and a_2 in the search interval $[t_1, t_2]$, so that the interval is divided into three sections $[t_1, a_1]$, $[a_1, a_2]$, $[a_2, t_2]$. Here,

$$\begin{aligned} a_1 &= t_2 - 0.618 * (t_2 - t_1) \\ a_2 &= t_1 + 0.618 * (t_2 - t_1). \end{aligned} \tag{14}$$

In this paper, we set the original search interval $[t_1, t_2]$ as $[0, 0.5]$. We first compare $J(a_1)$ and $J(a_2)$, and reset the search interval as $[t_1, a_2]$ or $[a_1, t_2]$. Repeat the above procedure in the newly generated interval until $\|t_2 - t_1\|$ is smaller than a threshold $e_{\min}$. In our experiments, we set $e_{\min} = 0.01$ from the accuracy consideration. Finally, $(t_2 + t_1)/2$ is used as the search step size $\alpha^{(t)}$.

Terminate Conditions: We set three termination conditions for the gradient descent search, and the iteration will be terminated if any of them is satisfied.

1) If the iterative times exceed a threshold $t_{\max}$, the iteration terminates. This is because the convergence rate drops rapidly when the iterative times become large. We want to terminate the iteration in limited steps. In this paper, we set $t_{\max}$ equal to 10.
2) If the Euclidean distance of two successive search locations $\|l^{(t+1)} - l^{(t)}\|$ is smaller than a predefined threshold $d_{\min}$, the iteration terminates. To make a fair comparison with the exhaustive search method, in this paper, we set $d_{\min}$ equal to 0.1 m.
3) If $l^{(t+1)}$ is outside of the target subarea, then the last iterative location $l^{(t)}$ is regarded as the estimated location.

The complete steps of gradient descent search are given in the following algorithm description.

Gradient Descent Search:
Input: J, $d_{\min}$, $t_{\max}$
Output: $\hat{l}(x, y)$, the estimated target location

$t = 0$
Get the initial location $l^{(0)}$
while $(t < t_{\max})$
  Compute the gradient $\nabla J(l^{(t)})$;
  Compute the search step $\alpha^{(t)}$;
  Compute the new location $l^{(t+1)}$;
  if $l^{(t+1)}$ is outside of the subarea
    $l^{(t+1)} = l^{(t)}$;
    break;
  if $\|l^{(t+1)} - l^{(t)}\| < d_{\min}$
    break;
  $t = t + 1$;
  Goto 3;
endwhile
return $l^{(t+1)}$

VI. Experiment Results

A. Experiment Setup

We conduct experiments in a typical office environment, the third floor of the State Engineering Laboratory for the Next Generation of Internet Access System in our university, which includes eight office rooms and one corridor. The total floor layout is of 16.2 m × 28.5 m large, and each room is of 6.8 m length and 6.9 m width. The thickness of one wall is 0.3 m. Fig. 2 plots the floor layout, where a 2-D coordinate system is used to describe the location of one point, and the origin point is chosen as the left-upper corner point of room 301. In our experiments, we deploy eight APs. The RPs are created according to the normal fingerprint technique by a grid approach. There are 25 evenly distributed RPs per room, each

Fig. 3. Part of the test office room. A tripod was used to hold a mobile phone for RSS samplings in the summer batch.

TABLE I
HIT RATE PERFORMANCE STUDY

No. of used RPs per room	6	10	15	20	25
Hit rate	94.87%	92.31%	93.59%	92.31%	93.59%
No. of used APs	4	5	6	7	8
Hit rate	92.31%	91.03%	94.87%	96.15%	93.59%

TABLE II
DISTANCE ESTIMATION ERROR STUDY

	AP1	AP2	AP3	AP4	AP5	AP6	AP7	AP8
CF AE	2.57	1.77	2.00	1.66	1.92	2.13	3.39	1.96
PM AE	4.50	4.17	4.98	5.16	12.42	4.80	6.45	3.35
CF ME	1.48	1.22	1.21	1.08	1.44	1.42	1.53	1.19
PM ME	2.08	1.38	2.46	2.13	3.04	3.91	2.26	2.11
CF SD	1.87	0.97	1.05	1.09	1.21	1.09	0.97	1.03
PM SD	4.85	2.50	4.40	3.03	2.87	13.80	2.47	2.10

separated by 1.6 m both horizontally and vertically. In addition, in total, 130 testing points were randomly selected.

We have conducted two batches of field experiments to test the proposed algorithms in the winter and summer seasons, respectively. The TP-Link TL-WR740N wireless routers were used as APs, and their locations are plotted in Fig. 2. Channel measurements of a WLAN at 2.4 GHz based on the 802.11g standard were conducted for RSS samplings. In each experiment batch, we conduct extensive field measurements to collect RSS samples for both RPs and testing points.

Fig. 3 shows a part of the test office room. In the winter experiment batch, a mobile phone is held by a person at the height of around 1.1 m, but there may have some slight height variations in between 1 and 1.2 m due to some posture change in the sampling phase. As the mobile is held by a person, the body blocking effect cannot be neglected. In the summer experiment batch, we use a tripod to hold a mobile phone at the height of 1.1 m. In both batches, however, we do not particularly specify the mobile orientation for RSS sampling. Furthermore, in the winter batch, a Xiaomi 1S mobile phone with Android 4.0 operating system was used for RSS sampling. In the summer batch, in addition to using a Xiaomi 1S, a Huawei U8860 mobile phone with Android 2.3 operating system was also used for RSS sampling. The reason of using two kinds of mobile devices is to cross test the proposed algorithms in different hardware platforms. In both batches, we did not control the people movement in each office room, and the flow of people was actually changing with time. Generally, during the office time, more people walked around and in/out the room, and during the lunch time, only our testers and an on-duty staff stayed in the room. In addition, the flow of people in summer was larger than in winter. In a short summary, our testing conditions were the same as everyday life in order to test our algorithms in realistic scenarios.

B. Experiment Results

We compare our proposed algorithms with the traditional fingerprint-based nearest neighbor algorithm with the use of subarea determination (denoted as SD-NN) and the traditional PM-based algorithms. In SD-NN, we first locate a mobile device into a subarea and then conduct the nearest neighbor algorithm in the selected subarea. For the PM-based algorithm, to make a fair comparison, we also combine it with the subarea division scheme. In each subarea, we calibrated the PM coefficients for each AP only based on RPs within the subarea. Our proposed CF-based algorithm can have three variations, and for the ease of presentation, they are simplified as the CF-ELS algorithm (CF and ELS), the CF-GLS algorithm (CF and GLS), and the CF-Lat algorithm (CF and lateration localization), respectively. Similarly, the PM-based localization can also be divided into the PM-ELS, PM-GLS, and PM-Lat algorithm.

1) Subarea Determination Performance: We first examine the subarea hit rate performance. The hit rate is defined as the ratio of the number of the correct subarea determinations divided by the total number of tests. Table I presents the subarea hit rate performance against the number of RPs per room (using eight APs) and the number of APs (using 25 RPs per room). It is observed that the average hit rate is above 91% under different conditions. Therefore, exploiting the natural division of the concrete walls to increase the fingerprint discrimination and making subarea determination are feasible in practical indoor environments.

2) Distance Estimation Performance: Table II compares the distance estimation performance of using CF and PM under fitting degree $m = 2$, respectively. AE, ME, and SD, represent average error, median error, and standard deviation, respectively, and the distance error is measured in meters. We average the distance estimation for each AP over all testing points. It is seen that the CF method can achieve more accurate distance estimations. In particular, the average distance estimation error for an AP is about 2 m by using the CF, whereas it is more than 4 m by using the PM method.

Then, we present an example of the constructed fitting function. For room 303, Fig. 4 plots the measurements and the fitting results about AP 1 by using the CF method and the PM method. In particular, when we set $m = 2$, the constructed CF function is as follows:

$$d = \Phi(s) = 0.001 \times s^2 - 0.0534 \times s + 2.9626.$$

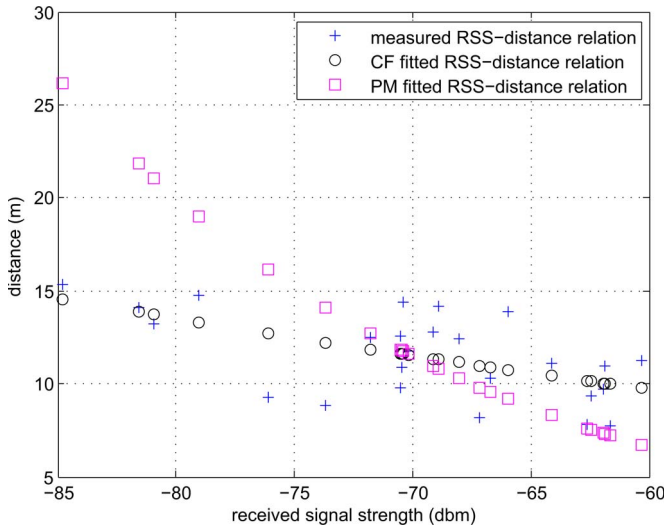

Fig. 4. RSS measurements and RSS fitting results.

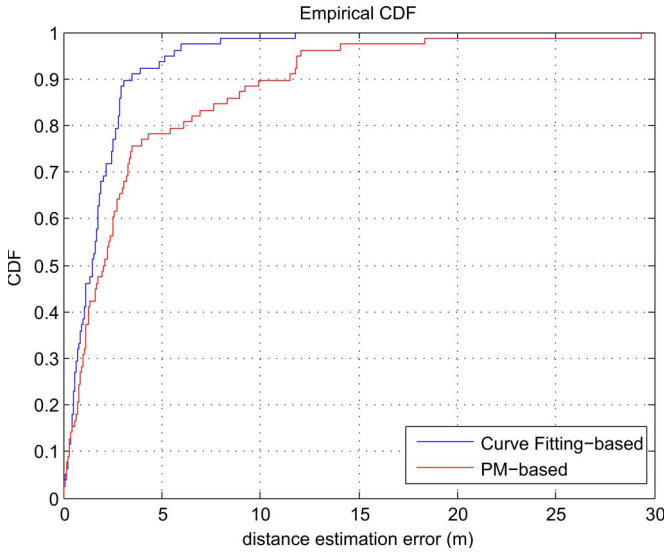

Fig. 5. Experiment results: The cdf of distance estimation error for AP 1 in room 303.

and the fitted PM function is given by

$$\mathrm{RSS} = -42.2780 - 10 \times 2.6653 \times \log(d).$$

In Fig. 4, we can see that the RSS–distance relation in indoor environment is quite complex. In particular, the signal propagation seems not to obey the log-distance path-loss model. Therefore, using the PM to estimate the RSS–distance relation may not be suitable in indoor environments and may lead to large localization errors. On the contrary, the CF method does not put such a constraint of log-distance path loss for the fitting function and can better reflect the basic change trend of these data for indoor environments.

Fig. 5 plots the cumulative distribution function (cdf) of the distance estimation error for AP 1. In this case, the CF method has a 29% improvement (from 2.08 to 1.48 m) compared with the traditional PM method in terms of the distance estimation accuracy.

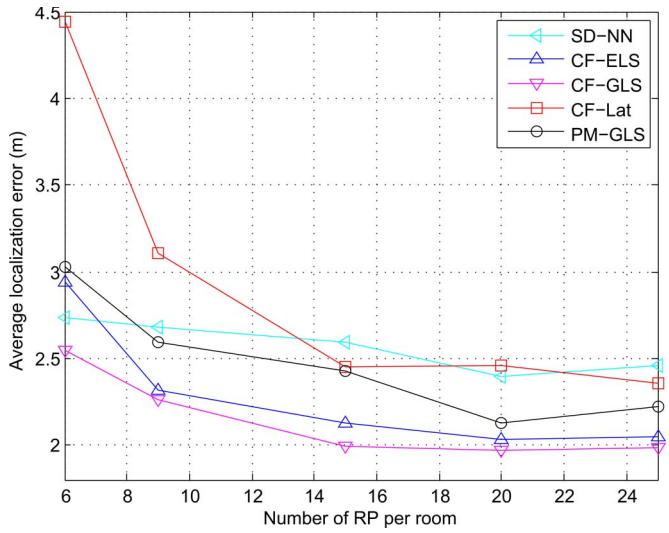

Fig. 6. Experiment results: Localization error versus the number of used RPs per room.

3) Localization Performance Study: In our experiments, the fitting degree m is set as 2. If we choose a large value for m, we have to use more RPs's fingerprints to avoid the overfitting phenomenon. However, using a large value of m would also require more RPs and their samplings, which increases the RSS sampling burden. Whereas for a small value of m, the fitted function could also reflect the basic signal change trend, although not accurate as a large value of m does sometimes. A small value of m only brings few fitting coefficients and introduces little computation during the positioning phase. To balance the accuracy and computation, we set m as 2 in all our experiments.

Fig. 6 plots the localization error against the number of used RPs per room.[1] In this figure, we do not include the PM-Lat and PM-ELS results as their performance are much worse than the CF-ELS and CF-GLS. All the three location search-based algorithms perform better than SD-NN, and the CF-GLS performs the best. In particular, the average improvement of CF-ELS and CF-GLS compared with the SD-NN algorithm are about 17% and 20%, respectively. This is not unexpected as the CF functions provide a reliable description of radio propagation characteristics, and the search space of the location search-based method is much larger than that of the NN algorithm of only a few of RP points. Second, it can be observed that both CF-ELS and CF-GLS perform better than the CF-Lat method. The average improvement are about 22% and 26%, respectively. The reason is that the lateration method performs well only with precise estimated distances. Note that, due to the complex indoor environment and the limited RSS sensitivity of the mobile device (the signal strengths are quantized into discrete levels by the device [43]), the minimum localization error is 1.97 m in our field experiments.

Fig. 7 plots the localization performance when different numbers of APs are used. The AP selection is listed in Table III. It

[1]Unless specifically noted, all results are based on using all eight APs when comparing the effect of the number of RPs or based on using 25 RPs per room when comparing the effect of the number of APs.

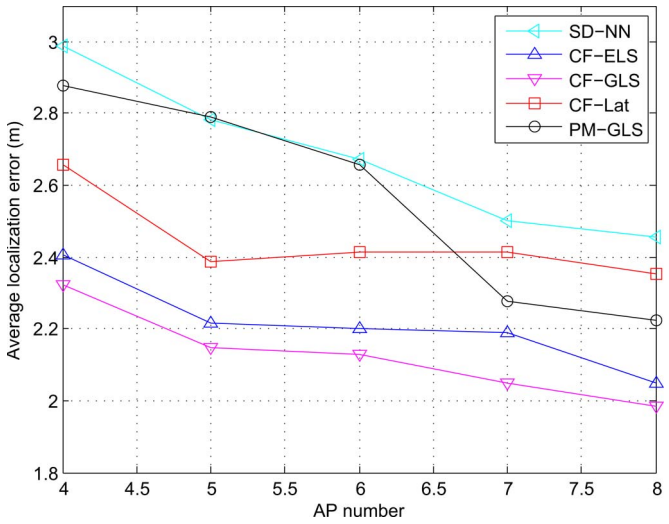

Fig. 7. Experiment results: Localization error versus the number of used AP.

TABLE III
APs USED IN THE LOCALIZATION

AP Number	AP Index	AP Number	AP Index
4	2,3,4,7	5	2,3,4,6,8
6	2,3,4,6,7,8	7	1,2,3,4,5,6,7

is first observed that the proposed CF-GLS algorithm achieves the lowest localization errors. Furthermore, with the increase in the number of used APs, the localization errors of the three algorithms decrease. The reason is that using more APs helps to increase the RSS fingerprint discrimination in between different RPs. Note that using fewer number of APs is time-saving and requires less computation. This indicates that there is a tradeoff between the number of APs and the localization accuracy when deploying a localization system.

We also did experiments to provide some insights on the relation between the number of RPs and the number of APs. Table IV gives the localization performance of our proposed CF-GLS method when changing the number of APs and RPs. From this table, we have some observations as follows. Generally, increasing the number of APs and RPs could help to improve the localization accuracy. This can be seen from each row and each column of the table. Second, we do not suggest using too few APs and RPs when positioning a mobile phone. For example, if only four APs and six RPs are used, the localization error can be as high as 2.85 m. To achieve desirable performance, it is necessary to ensure that either RPs or APs should be sufficient for fitting and positioning. Third, we find that the localization performance with 15 RPs used per room makes very little difference from that of with 25 RPs per room. This is due to the CF technique. By modeling the relation between RSS and distance with some RP fingerprints, the fitting functions provide a reliable description of radio propagation characteristics. Therefore, we do not have to collect too many fingerprints, thus reducing the training workload.

4) Localization Error Versus Different Devices: We then evaluate the proposed algorithms considering device heterogeneity. That is, the RPs are sampled using one device, and test points are sampled and positioned using another device.

TABLE IV
LOCALIZATION ERROR WHEN CHANGING THE NUMBER OF APS AND RPS FOR PROPOSED CF-GLS METHOD

	RPs=6	RPs=9	RPs=15	RPs=20	RPs=25
APs=4	2.8545	2.5836	2.3320	2.3663	2.3209
APs=5	2.5489	2.4663	2.2069	2.1561	2.1487
APs=6	2.4503	2.3256	2.1830	2.1416	2.1299
APs=7	2.5322	2.3319	1.9628	2.0801	2.0474
APs=8	2.5476	2.2611	1.9913	1.9729	1.9840

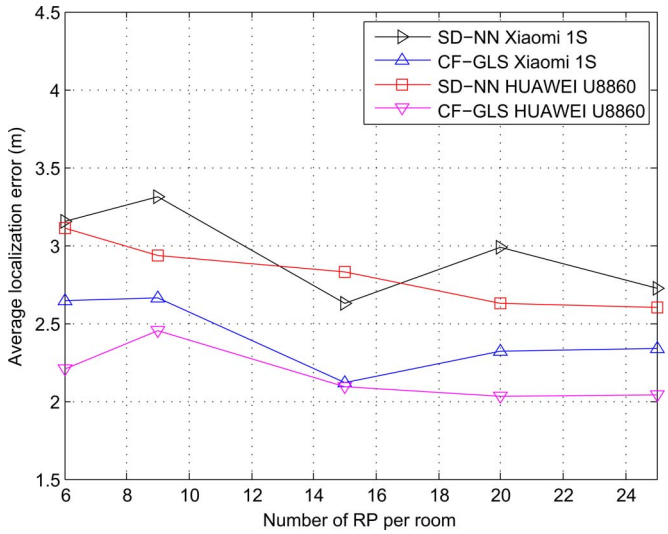

Fig. 8. Experiment results: Localization error versus the number of used RPs per room with different devices.

Fig. 8 compares the localization performance in the second experiment batch. We omit the PM-based methods as their localization performance are much worse than the presented ones. At first, we observe that the proposed CF-GLS method performs better than the traditional fingerprint-based method, even using different devices. Fig. 9 plots the cdf results when using six RPs per room. In particular, the improvement of localization accuracy against the SD-NN method is about 20% for Xiaomi 1S (from 2.90 to 2.33 m), and 29% for Huawei U8860 (from 2.86 to 2.03 m). Second, it is easy to find that the Huawei U8860 performs a little better than the Xiaomi 1S. This is because the Huawei U8860 is more steady for RSS sampling, as observed from our experiments.

5) Localization Error versus Environment Condition Change: In practice, the signal propagation environment is always changing, which may result in RSS fluctuations, as shown in Fig. 1. The ability of tolerating RSS fluctuations is one of the important performance indexes for an RSS-based indoor localization system. In this section, we evaluate the robustness performance of our proposed algorithm when the environment conditions change. As aforementioned, our two experiment batches are separated almost half a year, and one was in winter and another in summer. Here, we perform two group evaluations. In the first group, the RPs' RSS values sampled in winter are used for fingerprinting and CF, and in the second group, the RPs' RSS values sampled in summer are used. For two groups, we compare the localization performance using the testing points sampled in both winter and summer.

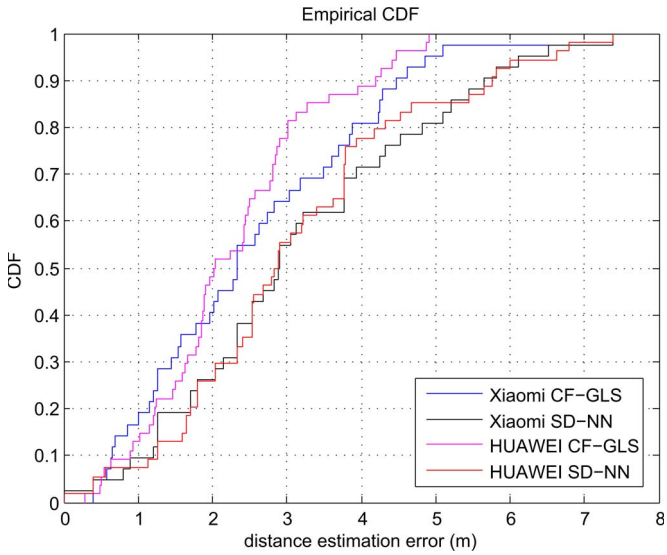

Fig. 9. Experiment results: The cdf of localization error under different device types when using six RPs per room.

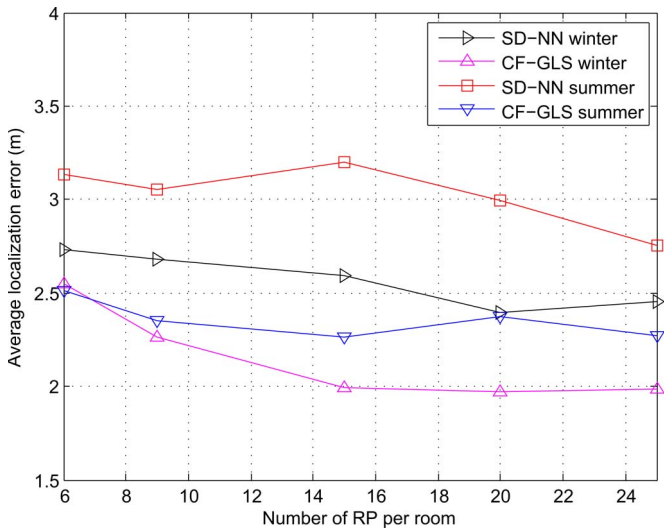

Fig. 10. Experiment results: The RPs' RSS samples in the first batch (winter) are used for fingerprinting and CF. The curve legends "winter" and "summer" indicate that the test points sampled in winter and summer, respectively, are used for localization.

In Figs. 10 and 11, it is shown that the CF-GLS method is less sensitive to the environmental change than the traditional fingerprinting-based method. In Fig. 10, the RPs are sampled in winter, but for the CF-GLS algorithm, its localization performance of using summer samples of testing points is not much degraded than that using winter samples. Furthermore, when using RPs and test points not sampled in the same season, the CF-GLS still performs better than the SD-NN method, even the SD-NN using RPs and test points sampled in the same day. In particular, take using 25 RPs per room for example; in Fig. 10, the localization error of SD-NN winter is 2.46 m, but the CF-GLS summer is 2.27 m. The performance improvement is about 8%. In Fig. 11, the localization error of SD-NN summer is 2.72 m, whereas CF-GLS winter is 2.40 m. The performance improvement is about 12%.

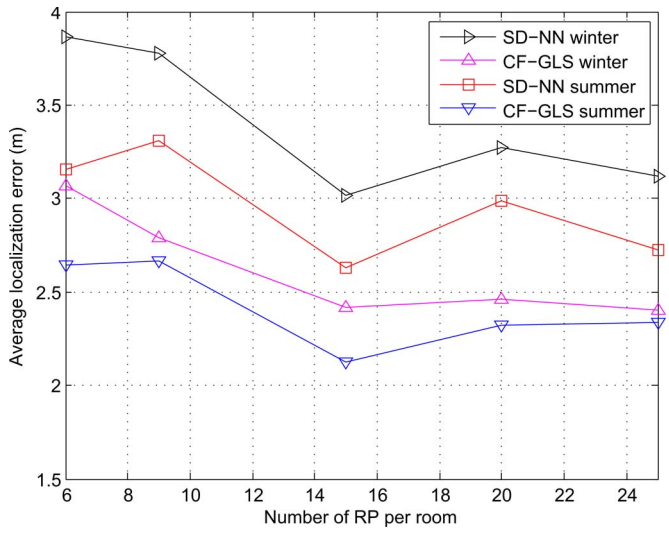

Fig. 11. Experiment results: The RPs' RSS samples in the second batch (summer) are used for fingerprinting and CF.

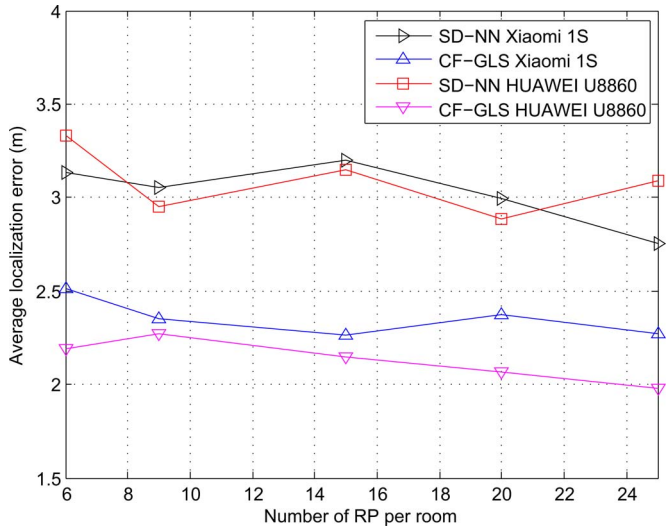

Fig. 12. Experiment results: Localization performance comparison using different devices. Where the RPs were sampled in winter, and test points were sampled in summer by two different devices.

If we further compare the "CF-GLS winter" of Fig. 10 and the "CF-GLS summer" of Fig. 11, it can be found that the performance of the former is better than the latter. As aforementioned, in the winter batch, a person held a mobile phone to do RSS samplings and the RSS measurements were affected by body blocking effect. However, the flow of people is more often in the summer batch than in the winter batch. This result might indicate that, compared with the human body blocking effect, the experiment environment plays a more important role on localization performance.

Then, we use different devices to further study the robustness of our method. Test points sampled in summer by the two devices are used to conduct localization. In Fig. 12, we can find that the CF-GLS method shows a great advantage than the SD-NN method for both two devices in different environment conditions. The average localization errors of CF-GLS are between 2 and 2.5 m, and those of SD-NN are between 2.75 and

3.3 m. The average performance improvements are between 24% and 27%. In short, the experiment results indicate that the CF-GLS method is more robust than the traditional fingerprinting-based method, in terms of graceful performance degradation in different environment conditions and heterogeneous devices types.

C. Complexity Discussion

Finally, we discuss the complexity of our proposed method and the traditional fingerprinting method. For the classic NN localization, its complexity is $O(N)$, where N is the total number of fingerprints to be compared in a given indoor environment. After applying the subarea division, the complexity of SD-NN becomes $O(K + N_{\text{subarea}})$, where K is the total number of subareas, and N_{subarea} is the largest number of RPs in some subarea. In this paper, N_{subarea} is equal to N/K. Therefore, it can be seen that the subarea division can help to reduce complexity for the traditional NN method. For the ELS method, the complexity is also dependent on the largest number of grid points in some subarea, denoted by $O(K + N_{\text{grid}})$. Usually, N_{grid} is much larger than N_{subarea}. Therefore, the complexity of the ELS is higher than the NN. For the GLS method, we use $O(K + N_{\text{subarea}} + t_{\max} \times B)$ to denote its complexity, where B represents the complexity of finding the next search point when conducting the iterative search, i.e., the computation complexity from lines 4 to 11 in the GLS algorithm description. The complexity of the GLS method is higher than the SD-NN. Given the prominent improvement of GLS localization accuracy over the SD-NN, such moderately increased complexity may be acceptable.

VII. Conclusion

In this paper, we have proposed a novel indoor localization scheme based on CF and location search. By conducting subarea division and CF in each subarea, we can obtain more accurate RSS–distance relation for each AP. We have also proposed to use subarea determination and location search to first locate a mobile device to a subarea and then search a location within the subarea to minimize the sum of distance errors. Field experiment results show that more than 17% and 22% improvements of localization accuracy have been achieved, compared with the traditional fingerprinting method and lateration method, respectively. Furthermore, our proposed localization method is also quite easy to implement.

We close this paper with some discussions about future work. The test environment is a typical office scenario yet with a regular layout. In our future work, we will consider complicated indoor environment with irregular layout and develop more sophisticated subarea division and fingerprinting scheme.

References

[1] X. Luo, W. J. O'Brien, and C. L. Julien, "Comparative evaluation of Received Signal-Strength Index (RSSI) based indoor localization techniques for construction jobsites," *Adv. Eng. Inf.*, vol. 25, no. 2, pp. 355–363, Apr. 2011.

[2] P. Lin, Q. Li, Q. Fan, X. Gao, and S. Hu, "A real-time location-based services system using WiFi fingerprinting algorithm for safety risk assessment of workers in tunnels," *Math. Prob. Eng.*, vol. 2014, pp. 371 456-1–371 456-10, 2014.

[3] S. Y. Jeong, H. G. Jo, and S. J. Kang, "Fully distributed monitoring architecture supporting multiple trackees and trackers in indoor mobile asset management application," *Sensors*, vol. 14, no. 3, pp. 5702–5724, Mar. 2014.

[4] F. Schrooyen *et al.*, "Real time location system over wifi in a healthcare environment," *J. Inf. Technol. Healthcare*, vol. 4, no. 6, pp. 401–416, 2006.

[5] E. Inc., Ekahau Solutions for Healthcare, 2014, (accessed on May 4, 2014). [Online]. Available: http://www.ekahau.com

[6] L. Pei *et al.*, "Using inquiry-based bluetooth rssi probability distributions for indoor positioning," *J. Glob. Positioning Syst.*, vol. 9, no. 2, pp. 122–130, 2010.

[7] M. S. Bargh and R. de Groote, "Indoor localization based on response rate of bluetooth inquiries," in *Proc. ACM Int. Workshop Mobile Entity Localization Tracking GPS-Less Environ.*, 2008, pp. 49–54.

[8] S. J. Kim and B. K. Kim, "Dynamic ultrasonic hybrid localization system for indoor mobile robots," *IEEE Trans. Ind. Electron.*, vol. 60, no. 10, pp. 4562–4573, Oct. 2013.

[9] K. H. Choi, W.-S. Ra, S.-Y. Park, and J. B. Park, "Robust least squares approach to passive target localization using ultrasonic receiver array," *IEEE Trans. Ind. Electron.*, vol. 61, no. 4, pp. 1993–2002, Apr. 2014.

[10] S. Park and S. Hashimoto, "Autonomous mobile robot navigation using passive rfid in indoor environment," *IEEE Trans. Ind. Electron.*, vol. 56, no. 7, pp. 2366–2373, Jul. 2009.

[11] B.-S. Choi, J.-W. Lee, J.-J. Lee, and K.-T. Park, "A hierarchical algorithm for indoor mobile robot localization using rfid sensor fusion," *IEEE Trans. Ind. Electron.*, vol. 58, no. 6, pp. 2226–2235, Jun. 2011.

[12] E. DiGiampaolo and F. Martinelli, "A passive uhf-rfid system for the localization of an indoor autonomous vehicle," *IEEE Trans. Ind. Electron.*, vol. 59, no. 10, pp. 3961–3970, Oct. 2012.

[13] S. S. Saab and Z. S. Nakad, "A standalone rfid indoor positioning system using passive tags," *IEEE Trans. Ind. Electron.*, vol. 58, no. 5, pp. 1961–1970, May 2011.

[14] P. Yang, W. Wu, M. Moniri, and C. C. Chibelushi, "Efficient object localization using sparsely distributed passive rfid tags," *IEEE Trans. Ind. Electron.*, vol. 60, no. 12, pp. 5914–5924, Dec. 2013.

[15] E. DiGiampaolo and F. Martinelli, "Mobile robot localization using the phase of passive uhf rfid signals," *IEEE Trans. Ind. Electron.*, vol. 61, no. 1, pp. 365–376, Jan. 2014.

[16] P. Yang and W. Wu, "Efficient particle filter localisation algorithm in dense passive RFID tags environment," *IEEE Trans. Ind. Electron.*, vol. 61, no. 10, pp. 5641–5651, Oct. 2014.

[17] S. Venkatesh and R. M. Buehrer, "NLOS mitigation using linear programming in ultrawideband location-aware networks," *IEEE Trans. Veh. Technol.*, vol. 56, no. 5, pp. 3182–3198, Sep. 2007.

[18] I. Guvenc, C.-C. Chong, and F. Watanabe, "NLOS identification and mitigation for uwb localization systems," in *Proc. IEEE WCNC*, Mar. 2007, pp. 1571–1576.

[19] L. F. M. de Moraes and B. A. A. Nunes, "Calibration-free wlan location system based on dynamic mapping of signal strength," in *Proc. ACM Int. Workshop MobiWac*, 2006, pp. 92–99.

[20] S.-H. Fang, T.-N. Lin, and K.-C. Lee, "A novel algorithm for multipath fingerprinting in indoor wlan environments," *IEEE Trans. Wireless Commun.*, vol. 7, no. 9, pp. 3579–3588, Sep. 2008.

[21] S.-H. Fang and T.-N. Lin, "Principal component localization in indoor wlan environments," *IEEE Trans. Mobile Comput.*, vol. 11, no. 1, pp. 100–110, Jan. 2012.

[22] J. Wang *et al.*, "Robust device-free wireless localization based on differential RSS measurements," *IEEE Trans. Ind. Electron.*, vol. 60, no. 12, pp. 5943–5952, Dec. 2013.

[23] Y. Chen, J.-A. Francisco, W. Trappe, and R. P. Martin, "A practical approach to landmark deployment for indoor localization," in *Proc. IEEE SECON*, Sep. 2006, pp. 365–373.

[24] W. P. L. Cully, S. L. Cotton, W. G. Scanlon, and J. B. McQuiston, "Body shadowing mitigation using differentiated LOS/NLOS channel models for RSSI-based monte carlo personnel localization," in *Proc. IEEE WCNC*, Apr. 2012, pp. 694–698.

[25] J. Wang, Q. Gao, Y. Yu, H. Wang, and M. Jin, "Toward robust indoor localization based on Bayesian filter using chirp-spread-spectrum ranging," *IEEE Trans. Ind. Electron.*, vol. 59, no. 3, pp. 1622–1629, Mar. 2012.

[26] P. Bahl and V. N. Padmanabhan, "Radar: An in-building RF-based user location and tracking system," in *Proc. IEEE INFOCOM*, 2000, vol. 2, pp. 775–784.

[27] M. Bshara, U. Orguner, F. Gustafsson, and L. V. Biesen, "Fingerprinting localization in Wimax networks based on received signal strength measurements," *IEEE Trans. Veh. Technol.*, vol. 59, no. 1, pp. 283–294, Jan. 2010.
[28] C.-Y. Shih, L.-H. Chen, G.-H. Chen, E.-K. Wu, and M.-H. Jin, "Intelligent radio map management for future WLAN indoor location fingerprinting," in *Proc. IEEE WCNC*, Apr. 2012, pp. 2769–2773.
[29] S.-H. Fang, T.-N. Lin, and P.-C. Lin, "Location fingerprinting in a decorrelated space," *IEEE Trans. Knowl. Data Eng.*, vol. 20, no. 5, pp. 685–691, May 2008.
[30] B. Li, Y. Wang, H. Lee, A. Dempster, and C. Rizos, "Method for yielding a database of location fingerprints in WLAN," *Proc. Inst. Elect. Eng.—Commun.*, vol. 152, no. 5, pp. 580–586, Oct. 2005.
[31] Y. Chen and H. Kobayashi, "Signal strength based indoor geolocation," in *Proc. IEEE ICC*, 2002, vol. 1, pp. 436–439.
[32] S. Mazuelas *et al.*, "Robust indoor positioning provided by real-time RSSI values in unmodified WLAN networks," *IEEE J. Sel. Areas Commun.*, vol. 3, no. 5, pp. 821–831, Oct. 2009.
[33] S.-P. Kuo and Y.-C. Tseng, "Discriminant minimization search for large-scale RF-based localization systems," *IEEE Trans. Mobile Comput.*, vol. 10, no. 2, pp. 291–304, Feb. 2011.
[34] H. Cho and S. W. Kim, "Mobile robot localization using biased chirp-spread-spectrum ranging," *IEEE Trans. Ind. Electron.*, vol. 57, no. 8, pp. 2826–2835, Aug. 2010.
[35] A. Dhital, P. Closas, and C. Fernndez-Prades, "Bayesian filtering for indoor localization and tracking in wireless sensor networks," *EURASIP J. Wireless Commun. Netw.*, vol. 2012, no. 1, p. 21, Jan. 2012.
[36] X. Chai and Q. Yang, "Reducing the calibration effort for probabilistic indoor location estimation," *IEEE Trans. Mobile Comput.*, vol. 6, no. 6, pp. 649–662, Jun. 2007.
[37] R. W. Ouyang, A. K.-S. Wong, C.-T. Lea, and M. Chiang, "Indoor location estimation with reduced calibration exploiting unlabeled data via hybrid generative/discriminative learning," *IEEE Trans. Mobile Comput.*, vol. 11, no. 11, pp. 1613–1626, Nov. 2012.
[38] X. Chai and Q. Yang, "Reducing the calibration effort for location estimation using unlabeled samples," in *Proc. IEEE Int. Conf. PerCom*, Mar. 2005, pp. 95–104.
[39] S.-P. Kuo, B.-J. Wu, W.-C. Peng, and Y.-C. Tseng, "Cluster-enhanced techniques for pattern-matching localization systems," in *Proc. IEEE Int. Conf. MASS*, Oct. 2007, pp. 1–9.
[40] M. A. Youssef, A. Agrawala, and A. U. Shankar, "WLAN location determination via clustering and probability distributions," in *Proc. IEEE Int. Conf. PerCom*, Mar. 2003, pp. 143–150.
[41] Y. Mo, Z. Cao, and B. Wang, "Occurrence-based fingerprint clustering for fast pattern-matching location determination," *IEEE Commun. Lett.*, vol. 16, no. 12, pp. 2012–2015, Dec. 2012.
[42] Y.-C. Chang, "N-dimension golden section search: Its variants and limitations," in *Proc. IEEE 2nd Int. Conf. Biomed. Eng. Inf.*, Oct. 2009, pp. 1–6.
[43] B. Joshua, The Truth About 802.11 Signal and Noise Metrics 2004. [Online]. Available: http://n-cg.net/ncgpdf/WiFi_SignalValues.pdf

Bang Wang (M'07) received the B.Eng. and M.S. degrees from Huazhong University of Science and Technology (HUST), Wuhan, China, in 1996 and 2000, respectively, and the Ph.D. degree in electrical and computer engineering from the National University of Singapore, Singapore, in 2004.

He is currently an Associate Professor with the Department of Electronics and Information Engineering, HUST. He is a holder of one European patent, and the author/coauthor of two books and over 90 technical papers published in international journals and conference proceedings. His research interests include indoor localization and navigation, wireless sensor network localization and coverage issues, and resource allocation and optimization algorithms in wireless networks.

Shengliang Zhou received the B.Eng. degree in electronic and information engineering from Wuhan University of Technology, Wuhan, China, in 2011 and the M.S. degree from Huazhong University of Science and Technology, Wuhan, in 2014.

He is currently a Development Engineer with MEIZU Technology Company, Zhuhai, China. His research interests include indoor localization and tracking systems and wireless networks.

Wenyu Liu (M'08) received the B.S. degree in computer science from Tsinghua University, Beijing, China, in 1986 and the M.S. and Ph.D. degrees in electronics and information engineering from Huazhong University of Science and Technology (HUST), Wuhan, China, in 1991 and 2001, respectively.

He is currently a Professor and an Associate Dean with the Department of Electronics and Information Engineering, HUST. His current research interests include sensor networks, multimedia information processing, and computer vision.

Yijun Mo received the B.Eng., M.S., and Ph.D. degrees from Huazhong University of Science and Technology (HUST), Wuhan, China, in 1999, 2002, and 2008, respectively.

He is as an Associate Professor with the Department of Electronics and Information Engineering, HUST. He was a Visiting Researcher with The Hong Kong University of Science and Technology, Hong Kong, in 2008. His research interests include wireless networks, semantic networks and service composites, and multimedia communications.